OBSERVATION OF COSMOS-1408 DEBRIS CLOUD WITH THE TRACKING AND IMAGING RADAR SYSTEM

D. Cerutti-Maori[(1)], C. Carloni[(1)], J. Rosebrock[(1)], and J. Siminski[(2)]

[(1)]*Fraunhofer Institute for High Frequency Physics and Radar Techniques (FHR), Wachtberg, Germany, Email: delphine.cerutti-maori@fhr.fraunhofer.de*
[(2)]*ESA/ESOC, Darmstadt, Germany*

ABSTRACT

On 15 November 2021 COSMOS-1408 was shot by a Russian ASAT (Anti-Satellite) weapon. The generated fragmentation cloud endangered the life of several astronauts on board the ISS (International Space Station) as well as of many active satellites. ESA commissioned the Fraunhofer Institute for High Frequency Physics and Radar Techniques (FHR) to observe the fragmentation cloud with the space observation radar TIRA (Tracking and Imaging Radar). In order to monitor the debris cloud, a special spotlight BPE (Beam-Park Experiment) mode was used by the TIRA system. The antenna beam was oriented towards a fixed spot in the inertial reference frame, thus staring at the same spot on the orbit of the progenitor. In addition, the largest piece of debris was observed with the imaging radar of the TIRA system. The paper presents the results of the conducted measurements and examines the parameter distributions of the detected debris.

Keywords: Space debris, Radar, COSMOS-1408.

1. INTRODUCTION

COSMOS-1408 was destroyed by a Russian ASAT weapon test on 15 November 2021 releasing several thousands of pieces of debris endangering the ISS and diverse active satellites [1, 2].

The Fraunhofer FHR was commissioned by ESA to observe the fragmentation cloud with the space observation radar TIRA [3]. Three observations of the debris cloud were conducted in November 2021. On December 1st, the largest piece of debris according to the database of ESA was observed with the imaging radar of the TIRA system. The TLE (Two-Line Elements set) used for these observations were retrieved from the webpage of Space-Track [4]. Table 1 lists some parameters of the conducted measurements.

This paper presents the results of the observations. Section 2 introduces the observation mode used by the L-band radar of the TIRA system and examines the parameter distributions of the detected debris. The findings of the measurement performed with the imaging radar are shown in Section 3. Section 4 summarizes the investigations.

2. OBSERVATION OF THE FRAGMENTATION CLOUD WITH THE TRACKING RADAR

2.1. Observation mode and mode settings

2.1.1. Observation mode

A spotlight BPE was used to observe the debris cloud with the tracking radar of the TIRA system. During a spotlight BPE, the antenna pointing is corrected for the Earth rotation so that the antenna beam stares to a fixed spot in space during the measurement. To initialize the observation, an old TLE of COSMOS-1408 dated prior to the explosion was used. The TIRA system was switched on several minutes before the expected beam crossing of COSMOS-1408.

An unmodulated pulse of 1 ms was selected for the spotlight BPE. This waveform yields a range resolution cell of 150 km. The total range variation for the three conducted experiments was between 500 km and 1100 km (see Table 1). Taking the distance of 800 km as an average range, the antenna footprint is about 7 km wide. This corresponds to an observed volume of about 5500 km^3 (single resolution cell). Figure 1 shows the acquisition geometry. During pulse compression[1], the maximum admitted Doppler shift around the expected Doppler frequency was $\pm$500 Hz, which relates to a maximum range rate variation of $\pm$56 m/s around the expected range rate.

[1]Note that no matched filter bank was applied as the observation and processing filter were matched to the parameters of the progenitor (tracking radar data with one single range/Doppler resolution cell).

Proc. 2nd NEO and Debris Detection Conference, Darmstadt, Germany, 24-26 January 2023, published by the ESA Space Safety Programme Office
Ed. T. Flohrer, R. Moissl, F. Schmitz (http://conference.sdo.esoc.esa.int, February 2023)

Observation	Date	Time (UTC)	Type of observation	Range (km)	Duration
1	17.11.2021	14:38	Spotlight BPE	600-800	887 s ($\approx$ 15 min)
2	18.11.2021	15:46	Spotlight BPE	900-1100	582 s ($\approx$ 10 min)
3	25.11.2021	14:12	Spotlight BPE	500-750	1617 s ($\approx$ 27 min)
4	01.12.2021	12:39	Imaging		

Table 1. Conducted observations

Figure 1. Observation geometry (single resolution cell)

2.1.2. Processing

The current processing scheme is based on a single pulse detection without pulse integration. To get a low number of false alarms, which does not alter the detection rate, the probability of false alarm was chosen to be 5e-5 for all the observations. Keeping the false alarm rate and the resulting detection threshold constant between the observations enables a comparison of the achieved results.

In a future work, the data will be processed with a coherent detector to improve the current detection sensitivity. This will allow reducing the minimum size of the detectable objects with respect to the current processing.

As previously mentioned, the range varies between the different observations and also within a data acquisition. This corresponds to an SNR (Signal-to-Noise Ratio) variation of about 14 dB between the minimum and the maximum range. According to the used detection scheme, the minimum detectable object size changes within and between the experiments. For the conducted observations, the range variation causes a change of the minimum detectable object diameter of about 2 cm (NASA SEM (Size Estimation Model) with the parameters of the TIRA system, Rayleigh scattering regime).

2.2. Detected debris

Table 2 summarises the number of detections for the conducted experiments. As expected from the radar equation [5, 6], the highest detection rate is obtained for the observation with the shortest range.

2.2.1. RCS over time

Figure 2 shows the measured RCS (Radar Cross Section) of the detected debris over time for the three observations. The beam crossing time of a debris is around 1-2 s. Consequently, the same debris can be detected several times, while it passes through the antenna beam. Multiple detections of the same debris have been clustered into one single detection.

A uniform detection distribution over the observation time can be observed for all the measurements. The detection rate is similar at the beginning and at the end of the data acquisition. It was neither possible to observe the leading part nor the trail of the debris cloud. Already two days after the fragmentation, the debris cloud was very extended. The cloud spreading was at least larger than $\frac{15\text{min}}{93\text{min}} \approx \frac{1}{6}$th of the orbit.

Figure 2 indicates that a large number of small debris (around -30 dBsm and below) crossing the beam could be detected. The different detection rates for the three observations can be explained by the different ranges.

2.2.2. Time between detections

The distribution of the time interval between two successive detections is shown in Figure 3. The distributions are similar for the three observations. The duration between two successive detections is generally below 10 s.

2.2.3. RCS distribution

Figures 4 and 5 show the RCS distribution in dBsm and in square meters, respectively. The figures reveal that the fragmented pieces have small RCSs. The minimum detection size is different for the conducted observations. This is caused by the different observation geometries.

Date	Number of detections	Number of false alarms	Range (km)	Duration of the observation	Detection rate
17.11.2021	86	∼0.6	600-800	887 s (≈ 15 min)	5.8 detections/min
18.11.2021	52	∼0.4	900-1100	582 s (≈ 10 min)	5.4 detections/min
25.11.2021	161	∼1.1	500-750	1617 s (≈ 27 min)	6.0 detections/min

Table 2. Detected debris

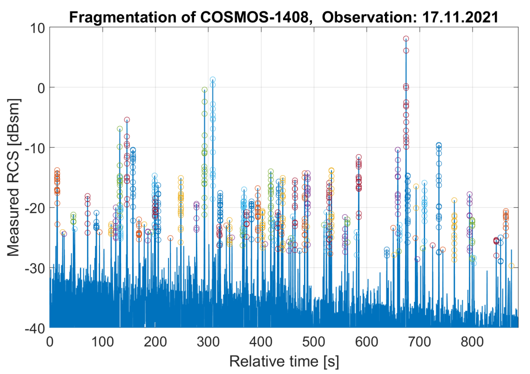

(a) 17.11.2021

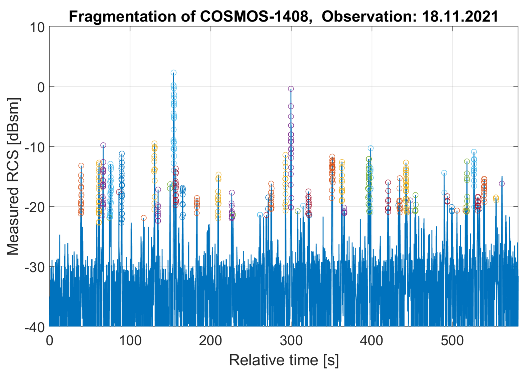

(b) 18.11.2021

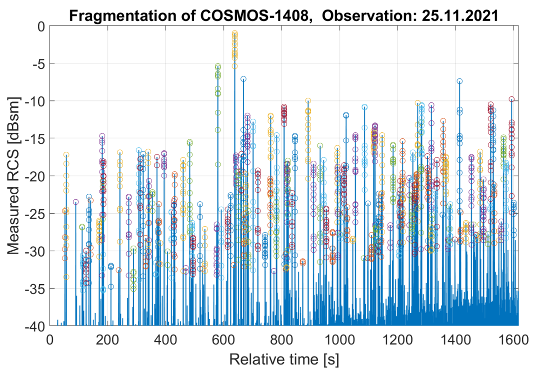

(c) 25.11.2021

Figure 2. RCS over time

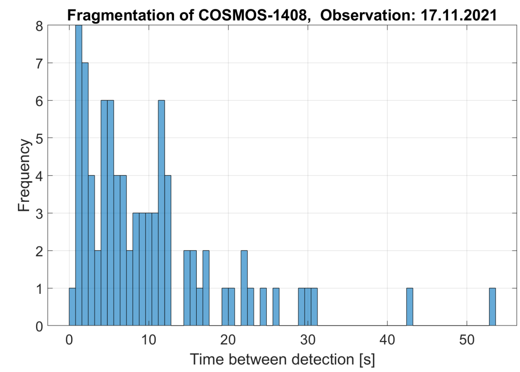

(a) 17.11.2021

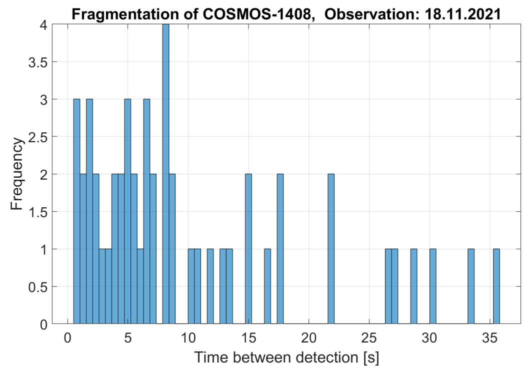

(b) 18.11.2021

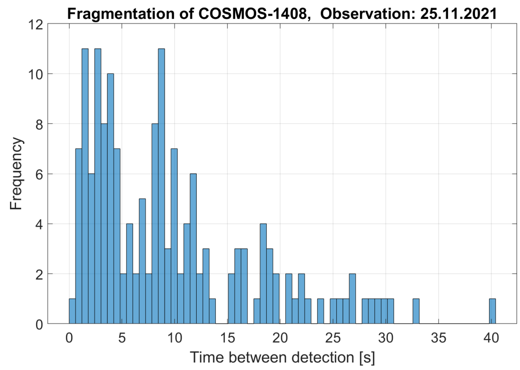

(c) 25.11.2021

Figure 3. Distribution of the duration between two successive detections

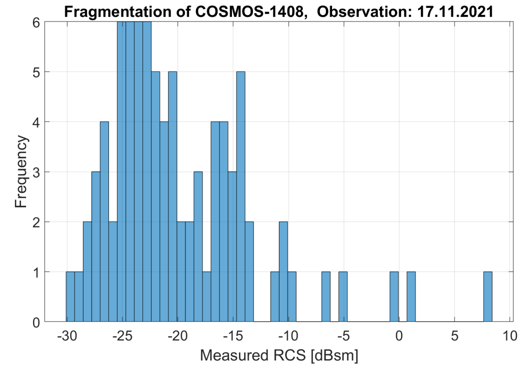

(a) 17.11.2021

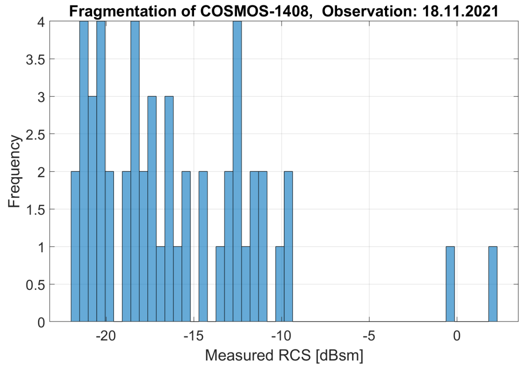

(b) 18.11.2021

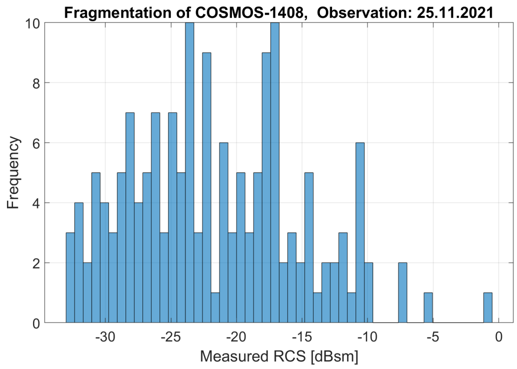

(c) 25.11.2021

Figure 4. RCS distribution (dBsm)

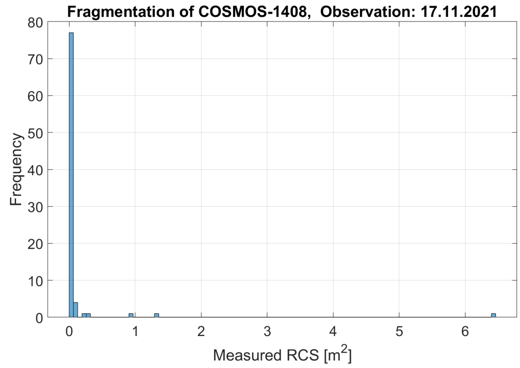

(a) 17.11.2021

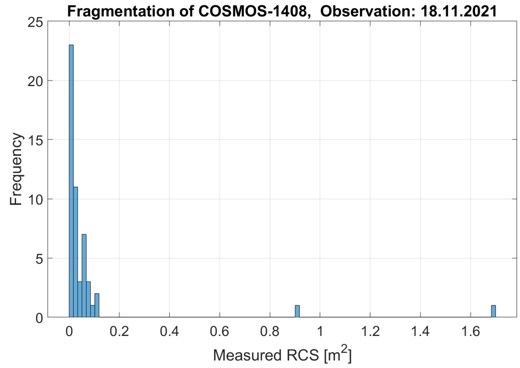

(b) 18.11.2021

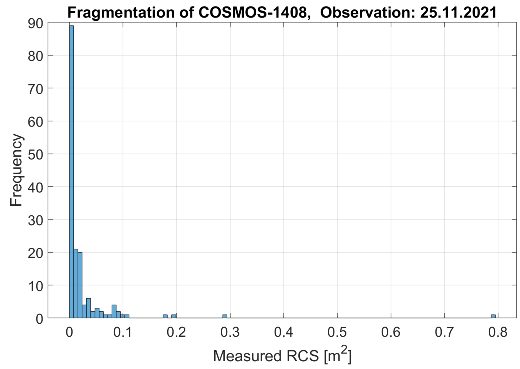

(c) 25.11.2021

Figure 5. RCS distribution (square meters)

2.2.4. Equivalent sphere diameter

Using the NASA SEM, an equivalent sphere diameter can be computed, which presents the same RCS as the measured one. The size distributions are shown in Figures 6 and 7. As already anticipated from the previous sections, the detected debris are small. Most of the objects are about 5 cm large (or smaller[2]) as indicated in Figure 7. Very few large pieces are present in the observed debris cloud. One large object with an equivalent diameter of about 3 m could be detected during the first observation. Another large object was detected during the second observation and another one during the last observation (see Figure 6). Due to the high variability of the RCS, it is not possible to determine if these detections correspond to the same object.

2.2.5. Estimated orbital parameters

From the measured range, range rate, azimuth angle, and elevation angle of the detected debris, the semi-major axis can be estimated under the assumption of a circular orbit (Figure 8). The same assumption is used to compute the Doppler inclination in Figure 9. Figures 8 and 9 reveal that the detected debris have similar inclination, eccentricity, and semi-major axis as their progenitor COSMOS-1408.

2.2.6. Extrapolated number of objects

Since similar detection distributions and detection rates were observed for the first (17 November) and the last observation (25 November), we can speculate that the debris cloud was already mostly uniformly distributed over the entire orbit 2-3 days after the fragmentation event. This is in line with previous modelling and observations [7]. From the orbital period (93 min) and the detection rate (6 detections/min), the number of debris larger than about 3-4 cm orbiting closest to the original orbit of COSMOS-1408 can be extrapolated and should count around 560 pieces.

It is important to note that the used observation mode is a spotlight mode, which solely focuses on a small region (150 km in range $\times$ 7 km in cross range) of the orbit of the progenitor. Fragmentation debris outside this observation window cannot be detected as they do not cross the main beam of the antenna pattern and of the ambiguity function. This explains why the number of trackable pieces detected by phased-array radars [8, 9] and other sensors [10] is higher compared to the extrapolated number of debris derived in this paper, although the size of the trackable fragments is much larger compared to the dimension of the debris detected by the TIRA system. In order to observe the whole debris cloud, a standard BPE

[2]Due to the truncation of the distributions, this fact cannot be verified but could be true.

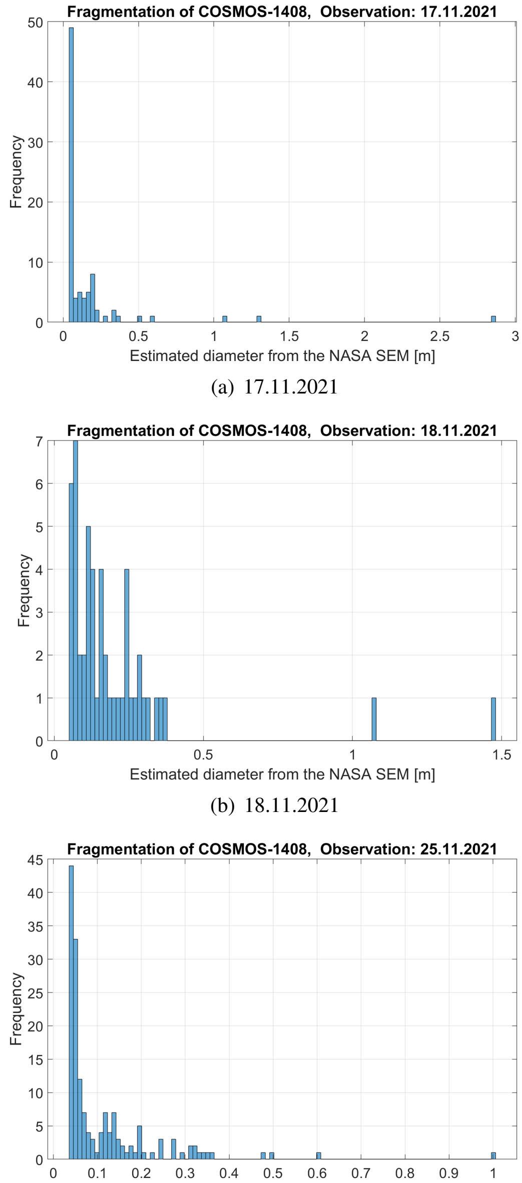

(a) 17.11.2021

(b) 18.11.2021

(c) 25.11.2021

Figure 6. Estimated size from the NASA SEM

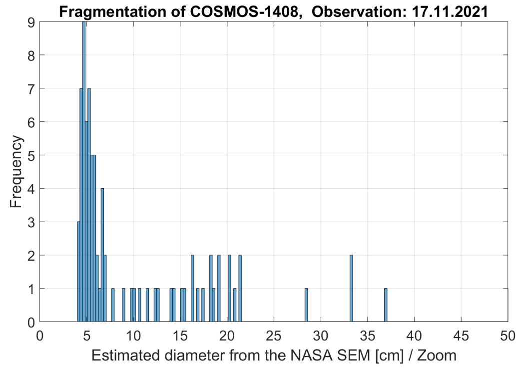

(a) 17.11.2021

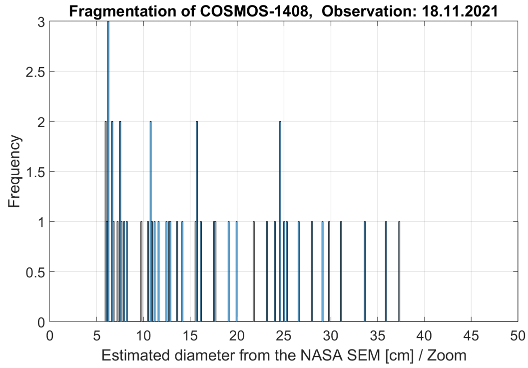

(b) 18.11.2021

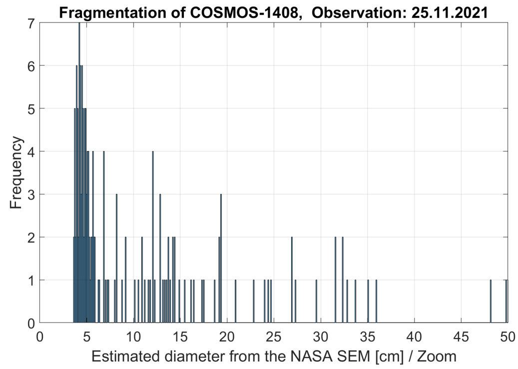

(c) 25.11.2021

Figure 7. Estimated size from the NASA SEM (Zoom)

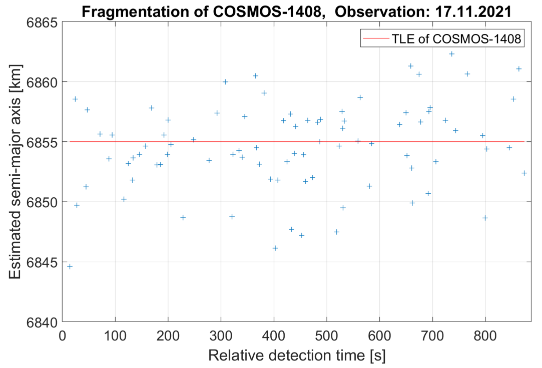

(a) 17.11.2021

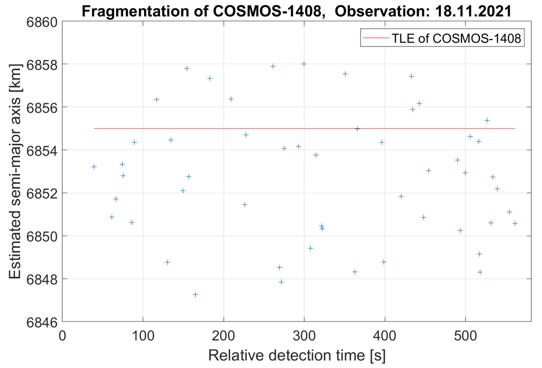

(b) 18.11.2021

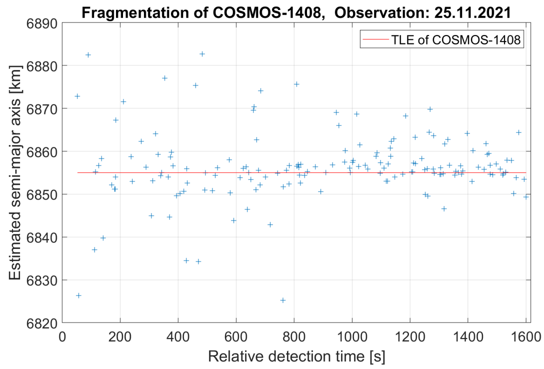

(c) 25.11.2021

Figure 8. Estimated semi-major axis

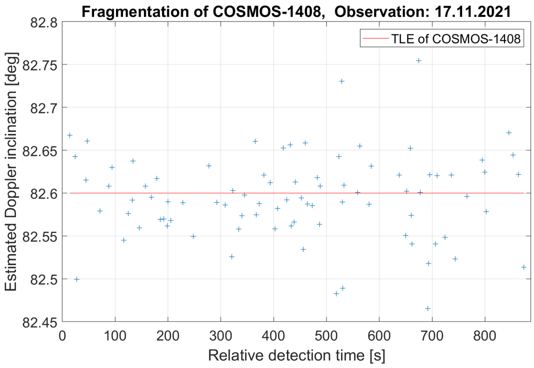

(a) 17.11.2021

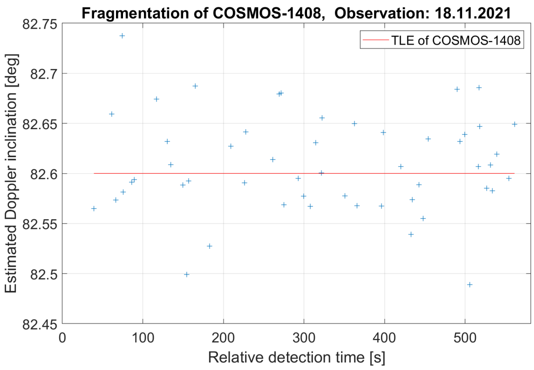

(b) 18.11.2021

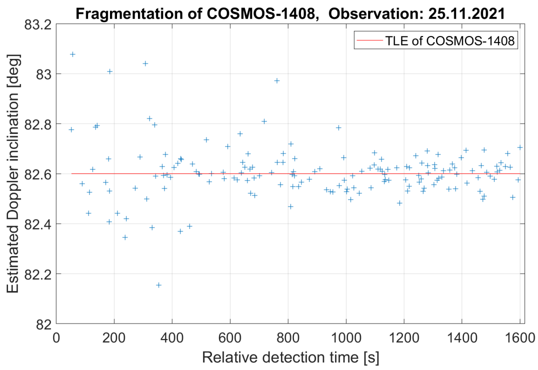

(c) 25.11.2021

Figure 9. Estimated Doppler inclination

Figure 10. Tselina-R (from [2])

mode [11] should be used. Trough the observation of a larger range/Doppler region and the Earth rotation, the whole fragmentation cloud could be potentially observed.

3. OBSERVATION OF THE LARGEST DEBRIS WITH THE IMAGING RADAR

According to [1], COSMOS-1408 was an ELINT (Electronic Signals Intelligence) satellite, which was part of the Tselina-D system for detailed observations. Figure 10 shows a picture of Tselina-R, which is an upgraded version of the Tselina-D satellite [12]. The shape of Tselina-D should be probably similar [2]. Information about the dimension of COSMOS-1408 could not be found. Reference [13] mentions that "*Tselina-2 basically is an enlarged version of Tselina-D. Its pressurized bus is 4.46 m high with a diameter ranging from 1.2 to 1.4 m*". The bus dimensions of COSMOS-1408 should be therefore about 4.5 m $\times$ 1.2-1.4 m or smaller, assuming the rightness of [13].

Figure 11 presents the obtained RTI (Range-Time Intensity) plot computed from the radar data acquired with the imaging radar of the TIRA system. The plot shows the obtained range profiles for some selected radar pulses. It is plotted in dB. A clear repeating pattern can be observed. The pattern (see the region between 206 s - 210 s) is replicating every 4 s. The pattern indicates that the object is tumbling extremely fast. The rotation period is around 4 s, which relates to an angular velocity of about 90 deg/s. Due to the fast angular velocity, the data are strongly undersampled and it was not possible to compute radar images.

The figure reveals that the minimum length of the object is about 4.5 m (green annotation). This length corresponds to the length of the satellite projected along the

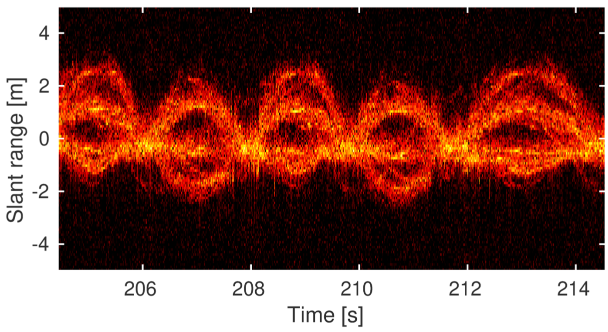

(a) RTI plot

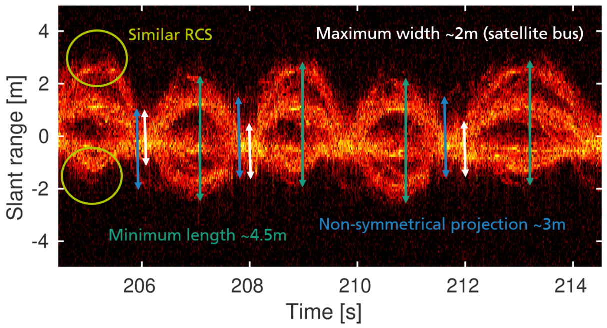

(b) RTI plot with annotation

Figure 11. RTI plot

LOS (Line Of Sight) direction. The RCS is similar at short and long range (yellow annotation), no specular reflection is observed. The main width of the object (including the cylinder-shaped bus and diverse remaining additional subsystems) is about 2 m (white annotation). The shape of the satellite is not symmetrical, as indicated by the non-symmetrical projection pattern (blue annotation).

Assuming a total satellite length of 4.5 m as for Tselina-2 [13], a possible interpretation is that the spin axis of the satellite could be perpendicular to the LOS direction during the observed time interval. Most of the satellite bus could be still intact. Part of the SIGINT (Signal Intelligence) detectors, that were attached to the four panels at the lower part of the satellite bus [13], were destroyed, as well as part of the solar panels. This explanation is, however, only a supposition in order to interpret the obtained RTI plot, without any guarantee about its correctness.

4. CONCLUSION

Several observations were conducted with the TIRA system to follow the temporal evolution of the fragmentation cloud, which was created by the destruction of COSMOS-1408 during a Russian ASAT weapon test on 15 November 2021.

In this paper, the results of three observations conducted with the tracking radar of the TIRA system between two days and ten days after the event were presented. Several parameter distributions of the detected debris were shown such as their RCS, the time between successive detections, the estimated debris size, and the estimated orbital parameters. The measurements indicated that most of the fragments were about 5 cm large or smaller.

Two weeks after the fragmentation, the largest piece of debris was observed with the imaging radar of the TIRA system. It was found that the debris was rotating very fast with an angular velocity of about 90 deg/s. Although the rotational velocity was too fast to compute radar images due to under-sampling in slow time, several information could be derived from the radar data such as the estimated dimension of the fragment. The radar data revealed that most of the satellite bus could be still intact.

ACKNOWLEDGMENTS

The authors would like to thank ESA/ESOC for funding this activity (Contract No. 4000127260/19/D/SR).

REFERENCES

1. https://en.wikipedia.org/wiki/Kosmos_1408.
2. https://space.skyrocket.de/doc_sdat/tselina-d.htm.
3. D. Mehrholz: Radar techniques for the characterization of meter-sized objects in space, Advances in Space Research, Vol. 28. No. 9, 2001, doi: https://doi.org/10.1016/S0273-1177(01)00395-7.
4. https://www.space-track.org.
5. Merill I. Skolnik: Radar Handbook, McGraw-Hill Professional.
6. Mark A. Richards: Fundamentals of Radar Signal Processing, McGraw-Hill, Electronic Engineering.
7. D. Oltrogge,T. Kelso, and T. Carrico: Characterizing the India ASAT Debris Evolution Using Diverse Complementary Tools, AAS 19-889.
8. https://leolabs-space.medium.com/analysis-of-the-cosmos-1408-breakup-71b32de5641f.
9. https://leolabs-space.medium.com/part-ii-new-observations-on-cosmos-1408-breakup-3d8e5441f720.
10. https://www.eusst.eu/newsroom/eu-sst-confirms-fragmentation-cosmos-1408/
11. J. Rosebrock, L. Leushacke, and D. Banka: Radar Signal Processing for Space Debris Observation, Frequenz, 2002, doi: 10.1515/FREQ.2002.56.11-12.249.
12. https://en.wikipedia.org/wiki/Tselina_(satellite).
13. https://brushbeater.org/wpcontent/uploads/2018/11/radars.pdf.